Optics Communications 401 (2017) 35–39

Contents lists available at ScienceDirect

Optics Communications

journal homepage: www.elsevier.com/locate/optcom

Holographic fluorescence mapping using space-division matching method

Ryosuke Abe, Yoshio Hayasaki *

Center for Optical Research and Education (CORE), Utsunomiya University, 7-1-2 Yoto, Utsunomiya 321-8585, Japan

ARTICLE INFO

Keywords:
Incoherent digital holography
Fluorescence microscope
Three-dimensional imaging
Phase imaging
Optical tweezers
Nanoparticle

ABSTRACT

Three-dimensional mapping of fluorescence light sources was performed by using self-interference digital holography. The positions of the sources were quantitatively determined by using Gaussian fitting of the axial and lateral intensity distributions obtained from diffraction calculations through position calibration from the observation space to the sample space. A space-division matching method was developed to perform the mapping of many fluorescence light sources, in this experiment, 500 nm fluorescent nanoparticles fixed in gelatin. A fluorescence digital holographic microscope having a 60× objective lens with a numerical aperture of 1.25 detected 13 fluorescence light sources in a measurable region with a radius of ~20 μm and a height of ~5 μm. It was found that the measurable region had a conical shape resulting from the overlap between two beams.

1. Introduction

Incoherent digital holography technology based on self-interference [1–5] has recently advanced and now allows the detection of incoherent light sources, such as objects that emit florescence [4,6–9], objects illuminated by a mercury arc lamp via a band-pass filter [10], light emitting diodes (LEDs) and objects illuminated by LEDs [11–14], and natural light sources [15]. Various optical arrangements have been used, such as a wavefront-folding interferometer [1], a rotational shearing interferometer [2], a Sagnac setup [3,13], Fresnel incoherent correlation digital holography (FINCH) [5–8], optical scanning holography [4], a lateral shearing setup [10], a Mach–Zehnder setup [9,11], and a Michelson setup [12,14,15].

An incoherent digital holographic microscope for fluorescence imaging (fluorescence digital holographic microscope) is another new type of fluorescence microscope that is an important tool in biology for visualizing the locations of biological molecules and fluorescent nanomaterials. The fluorescence digital holographic microscope is a good match with an adaptive imaging technique that is useful for an imaging in scattering media such as a biological sample [12,16]. The main advantage of this type of microscope is the ability to detect a three-dimensional (3D) image with a small number of captured images in a short time without the need for laser scanning or sample movement. This results in a small exposure to excitation light, which suppresses the degradation of fluorescent subjects, a problem faced in typical biological applications. The short imaging time offers the ability to analyze the spatial dynamics of biological chemical reactions in addition to the temporal dynamics. Observation of the spatiotemporal dynamics of many fluorescence points is indispensable in analyzing biological phenomena.

In the work described in this paper, we demonstrated the 3D imaging of fluorescent objects using a fluorescence digital holographic microscope [9]. The microscope was based on a modified Michelson setup in which weak fluorescence emitted from nanoparticles in the form of two spherical waves formed interference fringes on a small area. The modified Michelson setup was composed of commonly available reflective optical parts showing little dependence on wavelength and polarization, for detecting weak and broadband fluorescence. The other important aspect of our research was to perform quantitative 3D mapping of multiple fluorescence points to determine their dynamics. This is an important advantage of digital holography. Our holographic microscope incorporated optical tweezers, which were used to control the position of the target fluorescent nanoparticle, and also to suppress Brownian motion [17,18].

We demonstrated 3D mapping of fluorescent nanoparticles using self-interference digital holography and a space-division matching method. The 3D positions of the fluorescent nanoparticles in the observation space were determined by using Gaussian fitting of the axial and lateral intensity distributions obtained from diffraction calculations. The 3D positions in the sample space were obtained from position calibration from the observation space to the sample space, which was performed in advance. A space-division matching method was developed to perform the mapping of many fluorescent nanoparticles, although the sample

* Corresponding author.
E-mail address: hayasaki@cc.utsunomiya-u.ac.jp (Y. Hayasaki).

http://dx.doi.org/10.1016/j.optcom.2017.05.025
Received 9 March 2017; Received in revised form 8 May 2017; Accepted 13 May 2017
0030-4018/

had a small number of fluorescent nanoparticles in the view of field in our previous research [9]. In this experiment, a sample containing 500 nm fluorescent nanoparticles fixed in gelatin was used. The 3D mapping of many fluorescent nanoparticles gave a measurable conical region with a radius of ~20 μm and a height of ~5 μm using our present holographic microscope with a 60× objective lens having a numerical aperture of 1.25.

2. Experimental setup

Fig. 1 shows the experimental setup, which was composed of a fluorescence incoherent digital holographic microscope and optical tweezers. In the microscope, excitation light was radiated onto a sample from a fiber-coupled ultraviolet (UV) light emitting diode (LED) with a center wavelength of 365 nm (FOLS-01, Craft Center SAWAKI) through a commercially available fluorescence filter cube (UV-1A, Nikon). The fluorescence from nanoparticles in the sample was made to self-interfere, via an interferometer, on an electron multiplying charge-coupled device (EMCCD) image sensor with 1024×1024 pixels whose size was $13\ \mu m \times 13\ \mu m$, a 16-bit dynamic range, and a frame rate of 8.9 frames per second (iXon^{EM}+DU888E, ANDOR). The gain and the shutter speed of the image sensor were set to 85 and 100 ms, respectively. The interferometer was composed of two concave mirrors with focal lengths of 400 mm and 500 mm, and interference fringes were obtained via axial shearing of two images from the two arms. The image sensor was located on the plane that was apart from the focal plane of the concave mirrors to obtain the interference fringes on the appropriate region within the coherence. This optical arrangement was selected in consideration of the weak fluorescence from the nanoparticles, because if the fluorescence light from the nanoparticle was given to the image sensor with the enlargement, it would have insufficient intensity to form interference fringes with high contrast and high signal-to-noise ratio on the image sensor. The interference fringes were formed by incoherent addition of the Fresnel lenses coding all object points. A hologram was obtained with a four-step phase shifting method using a piezoelectric transducer (P-751K001, Physik Instrumente) controlled by the analog output of a computer board (AD16-16(PCI)E, CONTEC). The shutter was also controlled by the digital output of the computer board. The sample stage was moved with a mechanical stage (SFS-60XYZ, SIGMA KOKI) and a piezoelectric transducer stage (FINE-501, SIGMA KOKI), which were controlled through a GP-IB computer board (GP-IB(LPCI)F, CONTEC). These stages were used not only for searching the measurement area in the sample but also for performing 3D calibration between the sample space and the observation space. In the observation space, interference fringes were formed by the magnified wavefronts from an object in the sample space on an image sensor, a complex amplitude (hologram) was obtained on the image sensor plane, and diffraction calculations for its reconstruction were performed.

In the optical tweezers, the beam from an Yb-fiber laser with a wavelength of $\lambda = 1070$ nm (YLM-10, IPG Photonics) was collimated and focused in a sample solution using a 60× oil-immersion microscope objective lens (OL) with a numerical aperture of $NA = 1.25$ (UplanFL, Olympus). The irradiation laser power at the sample was calculated as the product of the power measured before introducing the laser beam and the transmittance of the OL. The optical tweezers were used to deliver a target fluorescence nanoparticle to the desired position and suppress the Brownian motion in a single particle experiment. It is noted that the optical tweezers were not used in the multi-particle experiments described later.

The sample contained fluorescence nanoparticles fixed in gelatin. The fluorescence nanoparticles, with a diameter of 500 nm (coefficient of variation (CV) <3%), had an excitation wavelength of 360 nm and a fluorescence wavelength of 410 nm (Fluoresbrite® BB Carboxylate Microspheres, Polysciences). They were sandwiched with a microscope slide glass and a cover slip.

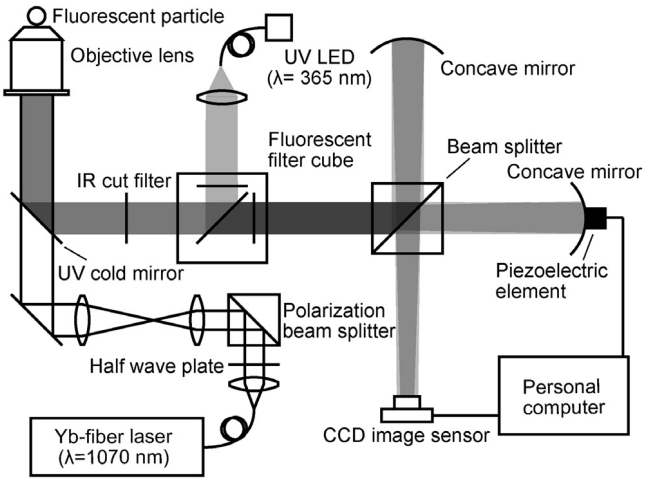

Fig. 1. Experimental setup. PBS, polarized beam splitter; HWP, half-wave plate; BS, beam splitter; OL, objective lens; PZT, piezoelectric transducer.

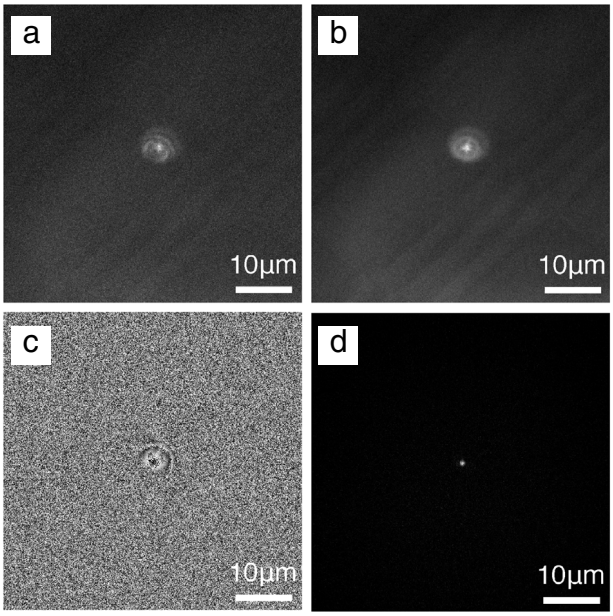

Fig. 2. (a) Interference fringes of a 500 nm florescence particles. (b) Amplitude and (c) phase of hologram. (d) Reconstruction on the focal plane.

3. Procedure of holographic mapping

3.1. 3D measurement of fluorescence nanoparticle

Fig. 2 shows fluorescence digital holography of a fluorescent nanoparticle trapped by the optical tweezers. One of the four interference fringes for the four-step phase-shifting method is shown in Fig. 2(a). The amplitude and phase of the hologram are shown in Fig. 2(b) and (c), respectively. The phase from 0 to 2π is shown by the gray scale. The reconstruction of the hologram with $z_{os} = 145$ mm in the observation space is shown in Fig. 2(d). The plane $z_{os} = 0$ mm is the hologram plane. The reconstruction was performed using the angular spectrum method [19]. In order to obtain the focal plane of each fluorescence point, the reconstruction was calculated with axial steps of Δz_{os}. The point with the strongest fluorescence intensity was sought from the diffraction images.

Fig. 3(a) shows the change of the peak fluorescence intensity along the axial direction. The focal plane was decided as follows. The axial